

Power Electronic Transformers for Utility Applications

Madhav D. Manjrekar

ABB Automation Inc.
16250, W. Glendale Drive
New Berlin, WI 53151
Ph: 262-780-3885
Fax: 262-780-3867

e-mail: madhav.manjrekar@us.abb.com

Rick Kieferndorf

University of Wisconsin-Madison
1415 Engineering Drive
Madison, WI 53706
Ph: 608-262-4479
Fax: 608-262-5559

e-mail: giri@engr.wisc.edu

Giri Venkataramanan

Abstract- A transformer is employed to perform several functions such as voltage transformation, isolation, noise decoupling and has been an indispensable component in power conversion systems. However, at low operating frequencies, it is one of the heaviest and the most expensive equipment in an electrical distribution system. The concept of realizing a small size “solid-state” transformer has been discussed for some time. A fairly straightforward approach to accomplish size reduction in a transformer feeding a conventional rectifier-inverter system is to introduce an isolated dc-dc converter in the dc link, isolation being provided by a high frequency transformer. So also, several topologies that employ ac-ac converters connected on primary and secondary sides of a high frequency transformer to reduce the size and weight of the magnetic core have been reported in literature. Such ac-ac converters need switches with bi-directional voltage blocking and current carrying capability, which are commonly realized with pairs of gate turn-off devices such as Insulated Gate Bipolar Transistors (IGBT). This paper explores the possibilities of employing ac-ac switched mode power converters in combination with reactive elements to realize a chopped ac link, thereby decreasing the required magnetic core size for voltage transformation and isolation. A primary advantage of this approach is that, the static power converter needs only six devices to implement a three-phase electronic transformer, which makes it an economical solution. Operating principles, magnetic design and other practical issues are discussed. Detailed computer simulations accompanied with experimental verification are presented in the paper.

I. INTRODUCTION

Since their inception at the turn of last century [1], transformers have been widely used in electric power conversion systems. The primary functions of a transformer are voltage transformation and isolation. Owing to the bulky iron cores and heavy copper windings in the composition, a transformer is one of the heaviest and most expensive parts in an electrical distribution system. The size and weight of a transformer is primarily a function of the saturation flux density of the core material and maximum allowable core and winding temperature rise [2]. The power throughput density is inversely proportional to frequency and hence increasing the frequency allows higher utilization of the steel magnetic core and reduction in transformer size [3], [4].

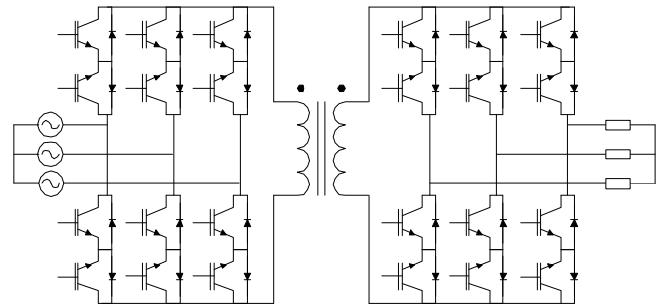


Figure 1. Power circuit schematic of a solid-state transformer employing a high frequency ac link stage.

The following section of this paper presents a brief survey of the state of the art in realizing solid-state transformers. Section III introduces the concept of Power Electronic Transformer (PET) derived from ac-ac buck-boost converter. The relative scaling properties of silicon and magnetic components used in the proposed PET technology are compared against the existing methods in Section IV. Simulation and experimental results verifying the performance characteristics of the proposed approach are presented in Section V. The paper concludes with a summary of results in Section VI.

II. STATE OF THE ART SOLID STATE TRANSFORMATION

A possible approach to introduce high frequency link is to use ac-ac frequency converters on both primary and secondary side exciting the transformer synchronously [5]. Figure 1 illustrates a simplified schematic of a three-phase transformer realized with this method.

As may be seen from Figure 1, the low frequency input sine wave voltage (60 Hz) is first converted to a high frequency ac link (typically a few kHz) by the primary side converter, which is then magnetically coupled to the secondary side. The isolated high frequency voltage is unfolded into a low frequency (60 Hz) waveform by the secondary side power converter. This operation requires both primary and secondary side static converters to operate synchronously, which is accomplished by modulating the switches by a high frequency square wave with 50% duty ratio. This is due to the fact that the transformer is purely an energy transformation device and instantaneous power

across the two-port input terminals is equal to that across the two-port output terminals. Since the transformer voltage contains only high frequency ac components, the resulting core size is small when compared to that which is designed for 60 Hz operation.

The static ac-ac converters in this topology employ bi-directional switches, which are realized by pairs of Insulated Gate Bipolar Transistors (IGBT) connected in series (Figure. 1). Hence, a total number of twenty-four devices are needed to realize a three-phase solid-state electronic transformer as shown, thus making it a rather cumbersome solution.

As an alternative, [3] presents an approach, which incorporates a high frequency link via an additional stage of dc-dc conversion methodology. A schematic of the approach is presented in Figure 2. The topology indicated in Figure 2 is adapted from [4] in order to provide bi-directional power flow feature and three phase operation.

As may be seen from Figure 2, the input ac voltage is rectified into dc using a switching power converter, which incorporates a boost type of rectifier, to maintain complete power control on the ac side including power factor control. The dc link voltage serves as the input to a full-bridge inverter, which synthesizes high frequency square wave pulses that are fed to an isolation transformer. The transformer secondary voltage is rectified, again using a bi-directional full bridge and then inverted using a three-phase bridge to synthesize a low frequency ac waveform. It should be mentioned that the power devices in the rectifier stage could be realized only using diodes if bi-directional power flow is not required.

The number of stages of power conversion in the dc link approach is readily evident from the schematic diagram. This contributes to reduced overall efficiency and high level of complexity.

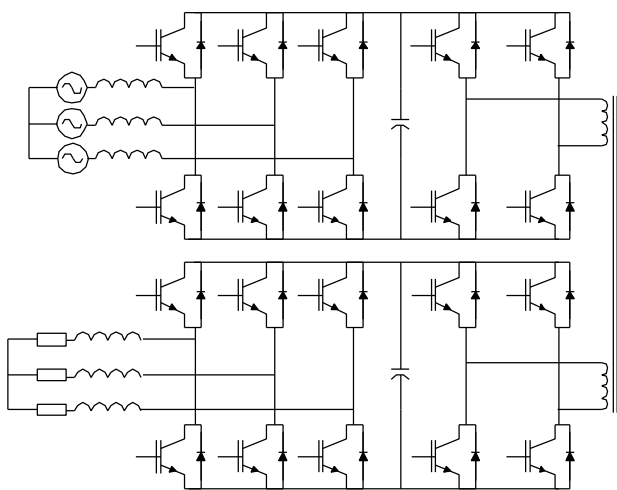


Figure 2. Power circuit schematic of a solid-state transformer employing an isolated dual dc link stage.

The trade-offs involved in the design and realization of these two approaches are more closely studied further in the paper.

III. POWER ELECTRONIC TRANSFORMER

This paper investigates the possibilities of employing ac-ac switched mode power converters in combination with reactive elements to realize a chopped ac link, thereby decreasing the required magnetic core size for voltage transformation and isolation. Several topologies of ac-ac direct converters have been studied in literature to solve problems related to power quality and to provide solutions for custom power [6]-[14]. Among these the buck-boost converter will be further investigated here for application as a solid-state transformer. Simplified power schematic of a representative ac-ac buck-boost converter is shown in Figure 3. As may be observed, this converter needs only six devices to accomplish three-phase power conversion. The output voltage is related to the input voltage through the duty ratio of the switching devices. The switches are operated under a Pulse Width Modulation (PWM) strategy at a duty ratio D . If V_i and V_o are defined to be the three dimensional vectors representing the input and output voltages, the transfer characteristics of the buck-boost converter may be represented as

$$V_o = \frac{D}{1-D} V_i \quad (1)$$

if the energy storage components are assumed to be small.

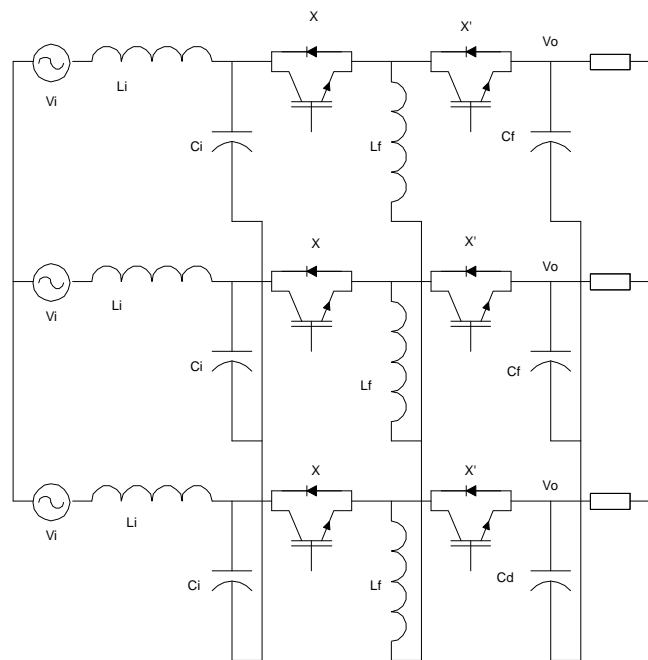


Figure 3. Simplified power circuit schematic of a three-phase ac-ac buck-boost converter.

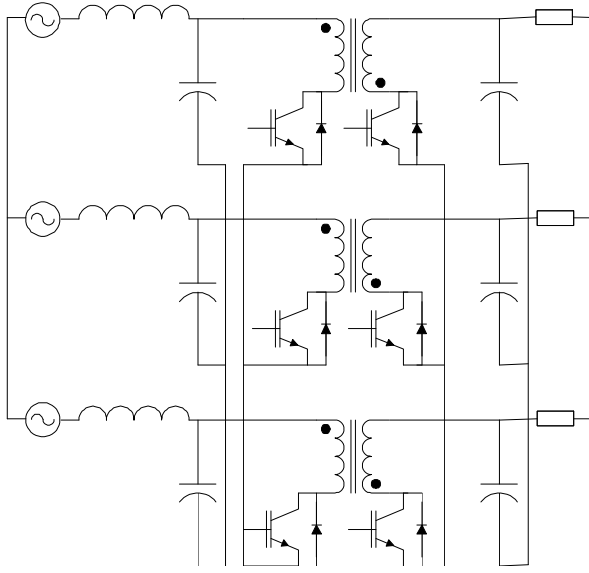


Figure 4. Simplified schematic of the proposed Power Electronic Transformer (PET).

The principle of operation of this converter is same as that of the corresponding buck-boost dc-dc converter. The input voltage (V_i) is applied across the energy storage inductor (L_f) when the switches labeled X are turned on. During this stage energy is transferred from the source to the inductor. During the complementary period, when the switches labeled X' are turned on, some of the energy stored in the inductor L_f is transferred to the output capacitor (C_f). The magnitude of the output voltage can be increased or reduced by means of duty cycle control [13], [14]. The inductor L_i and the capacitor C_i form a second order filter to reject harmonics in the input current from flowing into the source.

The proposed Power Electronic Transformer (PET) is constructed by replacing the energy storage inductor in the ac-ac buck-boost converter with a high frequency coupled inductor. A simplified power circuit schematic is illustrated in Figure 4. The ratio of turns of the windings on the primary and secondary side offers additional degree of freedom in determining the transfer characteristics. The dc-dc version of this topology is often termed as flyback converter.

IV. DESIGN CONSIDERATIONS

The design of semiconductors and reactive elements of the power electronic transformer follows the classical techniques using in the design of the dc-dc buck-boost or flyback converter [14].

The capacitive input filter and the output filter requirements of the ac link conversion approach and the

power electronic transformer are expected to be significant compared to the dc link conversion approach, because they both feature discontinuous input and output currents. On the other hand, the dc link based approach requires two sets of dc link capacitors, which have to supply discontinuous currents fed into the link by the switching matrix. Hence, in balance, the capacitive filtering requirements of all the three converters are expected to be of the same order of magnitude.

Studying the scaling properties of the main magnetic components of the three distinct approaches of realizing solid-state ac transformers illustrate important differences between them. The size of inductor is directly related to the energy storage capacity of the inductor. An estimate of their size may be developed based on the area product approach [15]. The area product represents the product of the cross sectional area of the core and the area of the window available for winding. The area product depends on the energy storage capacity of the inductor. The saturation flux density of the core and current carrying capacitor of the conductor determine the geometrical parameters that eventually result in the device of a certain size. The general expression for the area product of an inductor may be determined to be

$$WS = \frac{LI_p I_{rms}}{kB_{sat} J_{max}} \quad (2)$$

where k is the product of core stacking factor, winding fill factor, B_{sat} is the saturation flux density and J_{max} is the peak current density in the conductors. The value of the inductance L itself depends on the allowed ripple in the inductor. For a buck-boost converter operating at a nominal duty ratio of 0.5, the value of the inductance L may be determined using

$$L = \frac{V_{in}}{2F_s \Delta I} \quad (3)$$

where V_{in} is the input voltage, F_s is the switching frequency and ΔI is the current ripple. Combining equations (2) and (3),

$$WS_{bb} = \frac{V_{in} I_{rms}}{kB_{sat} J_{max} 2F_s} \frac{I_p}{\Delta I} \quad (4)$$

If $\Delta I/I_p$ is defined as per unit ripple factor δ , and P is defined as the VA rating of the power converter, the area product may be expressed as

$$WS_{bb} = \frac{P}{kB_{sat} J_{max} F_s \delta} \quad (5)$$

The factor of 2 in the denominator vanishes in this case, since the inductor current is twice the amplitude of the input

current in a buck boost converter. Equation (5) may be used to estimate the physical size of inductor in buck boost power converter in a compact manner, given its VA rating and the switching frequency. For the boost and buck converter, the area product of the inductor may be derived in a similar manner to be

$$WS_b = \frac{P}{2kB_{sat} J_{max} F_s d} \quad (6)$$

The area product of transformers related to their VA ratings and the operating frequency is well known and is given by [15]

$$WS_t = \frac{P}{kB_{sat} J_{max} F_s} \quad (7)$$

Based on the above expressions, the total area product required for the magnetic components of the three different approaches might be compared. The dc link based approach required two inductors per phase and one transformer. The buck-boost converter based approach requires one coupled inductor per phase. The ac link based approach requires one transformer.

The second important element that makes up the converters is the switching matrix. Silicon requirements of the converters may be compared by taking the summation of the product of voltage blocking requirements and current conduction requirements of various semiconductor devices utilized in the converter. For the buck-boost converter, it is well known that the switches need to block the sum of input voltage and the output voltage and each carry an average current equal to the input current. However, each switch conducts only one half cycle of the ac line current. Hence the total switch VA rating for the power electronic transformer operating at a nominal duty ratio of 0.5 happens to be,

$$VA_{bb} = \frac{4\sqrt{3}}{P} P \quad (8)$$

For the high frequency link transformer approach, the voltage ratings of the switches are at least equal to the line-to-line voltage of the input. The current rating of each switch is one third of the current in the link. Hence, the VA ratings for the switches may be calculated to be

$$VA_{aclink} = \frac{8\sqrt{3}}{P} P \quad (9)$$

In a similar manner, for the dc link based conversion approach, the VA ratings for the switches may be calculated to be

$$VA_{dclink} = 4\left(1 + \frac{\sqrt{3}}{P}\right)P \quad (10)$$

Figure 5 illustrates the variation of the total switch VA ratings of the three different approaches as the function of output power. The trade-offs involved in the three approaches are clear from the figure. From the circuit topological approach, one can notice the gradual increase in complexity progressing from the buck-boost converter towards the dc link based conversion approach. At low power levels, for the sake of keeping the silicon complexity and cost low, it is worth taking the penalty of larger size magnetic elements and choosing the power electronic transformer approach. However, as the power level increases, the penalty in magnetic elements becomes large enough that a high frequency link transformer based approach becomes attractive. At extremely high power levels, the distribution of stress and modularity offered by the dc link based approach becomes more attractive, in spite of the increased requirements on magnetic devices. It should also be noted that in cases where bi-directional power flow is not desired, the controlled switches in the rectifier bridges in the dc link based conversion approach may be eliminated.

It is also worth examining the locus of the transformer core flux in the three approaches. In the dc link based approach, the transformer experiences a classical square wave excitation at a high frequency as shown in Figure 6. The flux excursions are symmetrical and the BH curve follows a classical single loop. In the ac link based approach, as the line current progresses through the ac cycle, the excursions of the BH curve are still symmetrical, but the amplitude of the flux excursions follows the 60Hz ac waveform (Figure 7).

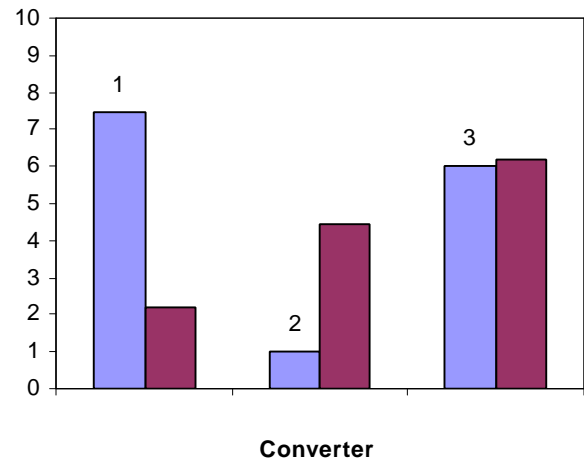


Figure 5: Illustration of relative size of magnetic elements (left bars) and power device kVA stress (right bars) for (1) Power Electronic Transformer (2) AC link conversion approach, and (3) DC link conversion approach

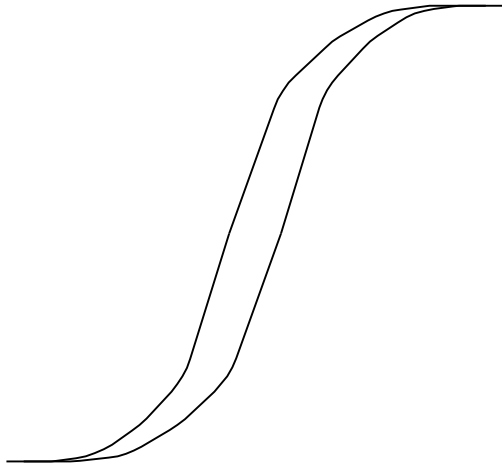


Figure 6: Typical B-H Trajectory in dc link conversion approach.

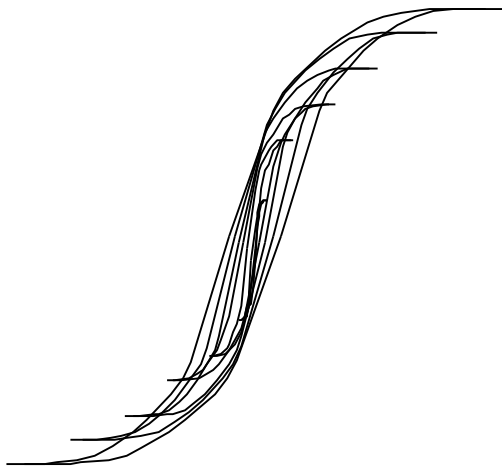


Figure 7: Typical B-H Trajectory in ac link conversion approach.

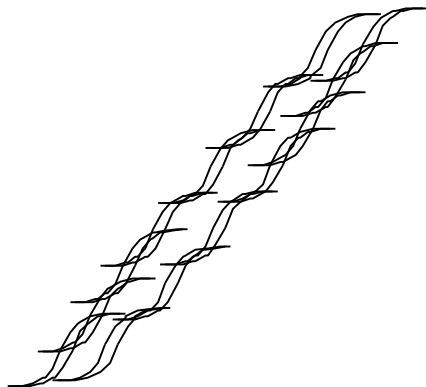


Figure 8: Typical B-H Trajectory in power electronic transformer.

In the coupled inductor of the PET, the flux excursions follow minor loops at a high frequency, while the center of the minor loops traverses a low frequency trajectory of the 60 Hz ac wave as shown in Figure 8. The models for core losses under such complex excitations are not widely available. However, the losses in the dc link conversion may be expected to be the highest, followed by the ac link

approach, with the PET approach having the lowest amount of core losses.

V. SIMULATION AND EXPERIMENTAL RESULTS

AC and DC link based solid-state transformers have been experimentally demonstrated and are being studied for various applications [3]-[5]. However, buck-boost converter based power electronic transformers have not been studied definitively in the past. Hence the operation of the converter was verified using simulation and laboratory prototyping. A detailed computer model of the converter was built using Matlab Simulink[®]. The parameters for the converter used in the simulation were: $L_f = 120 \mu\text{H}$, $C_o = 360 \mu\text{F}$, Load resistor = 15 Ohms. The input and output voltages were three-phase 230 V line-line rms. The transformer turns ratio was unity.

Simulation under various operating conditions has been extensively performed to verify the operation of the converter. The waveforms of input voltage, output voltage and inductor flux operating at 50% duty ratio are shown in Figures 9-11 respectively.

A small voltage drop between the input and output voltage can be observed between Figure 9 and Figure 10. This is due the voltage drop across the finite reactance of the energy transfer inductor at the power frequency. In a dc-dc converter, the dc average voltage across the inductor is zero. In ac-ac converters, the inductor have a finite (reactive) voltage drop across them, and so do capacitors which drawn reactive current at the power frequency. A Fourier spectrum of the transformer flux waveform is shown in Figure 12, illustrating the predominance of high frequency flux in the excitation.

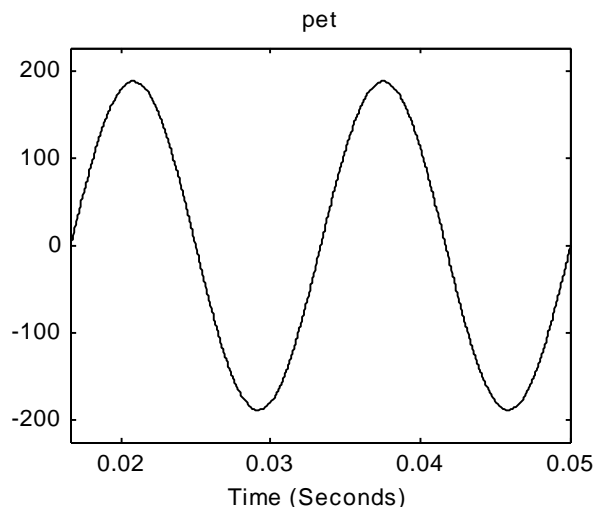


Figure 9. Typical input phase voltage waveform for the proposed power electronic transformer.

An experimental prototype converter rated at 10 kW was built to verify the feasibility of the approach. The converter utilized IGBT modules operating at 5 kHz

switching frequency. The coupled inductor was realized using toroidal power iron cores with a relative permeability of 33. Primary and secondary windings consisted of 25 turns of bifilar wound litz wires. Bifilar winding was used for minimizing the leakage reactance between the secondary and primary windings of the coupled inductor. The controller for generating the gate drive signals was implemented using a TI 320C240 digital signal processing system.

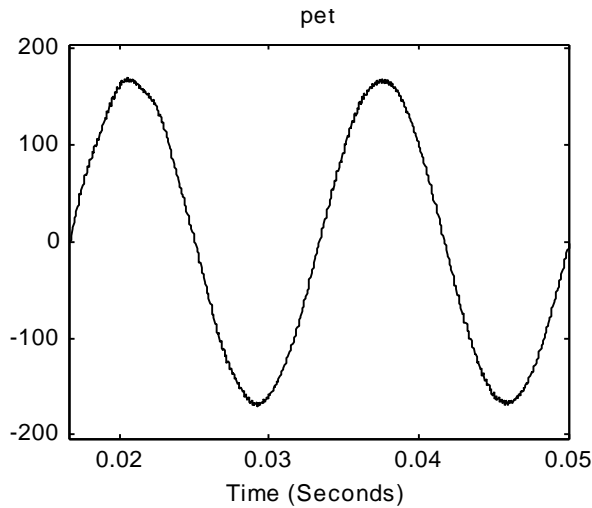


Figure 10. Typical output phase voltage waveform for the proposed power electronic transformer.

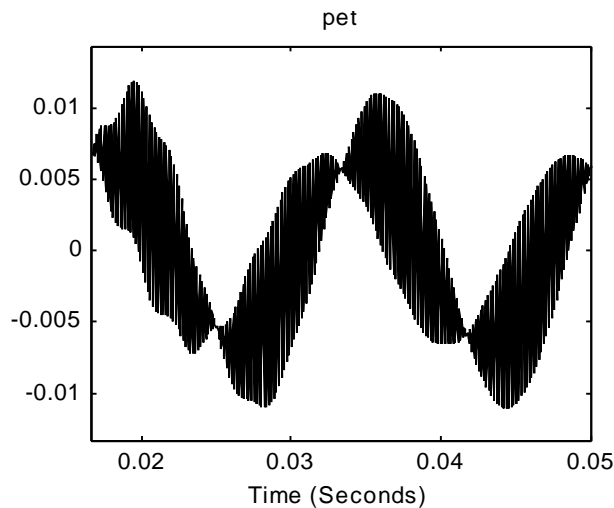


Figure 11. Typical transformer flux waveform for the proposed power electronic transformer.

Waveforms of output voltage, transformer voltage and inductor current are illustrated in Figure 13. A commutation algorithm for switching the devices that eliminates the dead time during transitions is being implemented. A closed loop voltage regulator that maintains output voltage regulation under varying line and load conditions is also being studied.

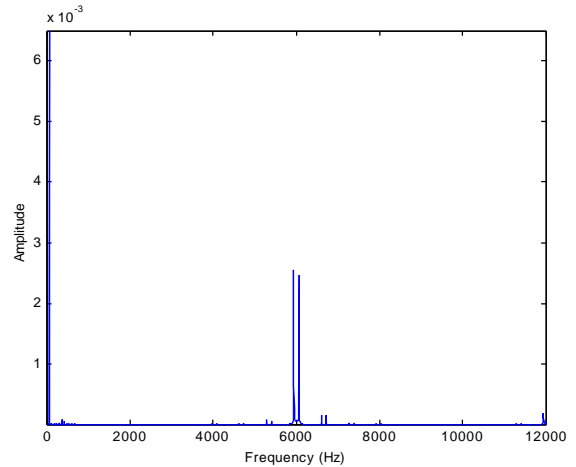


Figure 12. Typical transformer flux spectrum for the proposed power electronic transformer.

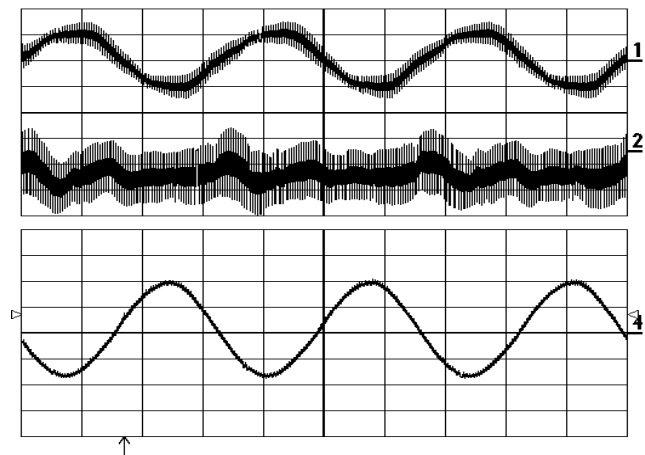


Figure 13: Experimental traces of inductor current (primary and secondary currents coupled together), inductor voltage and output voltage obtained from the laboratory prototype.

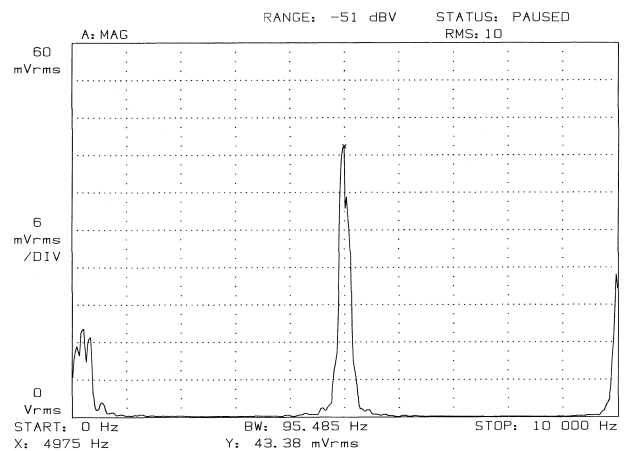


Figure 14: Spectrum of the sum of primary and secondary currents of the coupled inductor.

A spectrum of the inductor current (including the reflection of secondary side current to the primary side) is illustrated in Figure 14. The predominance of the high frequency excitation of the core is evident from the graph. Further characterizations of the prototype system to measure the efficiency, operation under varying load conditions are under way.

The dynamic model for the converter may be developed based on extension of state space averaging techniques to systems excited by periodic waveforms and will be reported in the future. These models form the basis for developing closed loop regulators for the system. The interaction of the system with the power system properties becomes important as the converter features an incremental negative resistance type of load to the system due to its regulatory properties. These issues are being studied and results will be presented as they unfold.

VI. CONCLUSIONS

This paper has presented a solid-state transformer based on the ac-ac buck-boost power electronic converter. The topology is a direct extension flyback dc-dc converter for three phase ac systems. Trade-offs involved in application of this topology in relation to other topologies such as the dc link and ac link conversion approaches have been presented. The proposed converter appears to be a competitive candidate for low power applications where simplicity of the power circuit hold paramount importance over other issues such as optimization of magnetic elements and power semiconductor elements. The operation of the power converter topology has been verified using simulations and experiments.

The field of ac-ac power conversion involving no frequency change represents an important field of application of power electronic systems. Such power conversion and control applications form the backbone of the electrical utility power systems. This paper has presented one more power converter that can be used for developing applications in the ac-ac power conversion.

ACKNOWLEDGMENT

Grateful thanks are due to Wisconsin Electric Machines and Power Electronics Consortium, and the University of Wisconsin-Madison Graduate School for providing support for the work described in this paper.

REFERENCES

- [1] Nikola Tesla, "System of Electrical Distribution," US Patent # 381970, 1888.
- [2] N. Mohan, T.M. Undeland and W.P. Robbins, *Power Electronics*, John Wiley and Sons, 2nd ed., 1995.

- [3] S. Sudhoff, "Solid State Transformer," US Patent # 5943229, 1999.
- [4] E. Ronan, S. D. Sudhoff, S. F. Glover and D. L. Galloway, "Application of Power Electronics to the Distribution Transformer," *Conference Record of APEC 2000*, New Orleans, February, 2000, pp. 861-867.
- [5] M. Kang, P.N. Enjeti and I.J. Pitel, "Analysis and Design of Electronic Transformers for Electric Power Distribution System," *Conference Record of the IEEE-IAS Annual Meeting 1997*, pp. 1689-1694, 1997.
- [6] Mozdzer Jr. and B.K. Bose, "Three-phase AC Power Control Using Power Transistors," *IEEE Transactions on I.A.*, Vol. 12, no. 5, 1976, pp. 499-505.
- [7] A.K.S. Bhat and J. Vithayathil, "A Simple Multiple Pulsewidth Modulated AC Chopper," *IEEE Transactions on I.E.*, Vol. 29, no. 3, 1982, pp. 185-189.
- [8] P.D. Ziogas, D. Vincenti and G. Joos, "A Practical PWM AC Controller Topology," *Conference Record of the IEEE-IAS Annual Meeting 1992*, pp. 880-887, 1992.
- [9] G. Venkataramanan et al., "AC-AC Power Converters for Distribution Control," *NSF Symposium on Electric Power Systems Infrastructure 1994*, pp. 159-162, 1994.
- [10] G. Venkataramanan, B. K. Johnson and A. Sundaram, "An AC-AC Power Converter for Custom Power Applications," *IEEE Transactions on Power Delivery*, July 1996.
- [11] G. Venkataramanan and B. K. Johnson, "A Pulse Width Modulated Power Line Conditioner for Sensitive Load Centers," *IEEE Transactions on Power Delivery*, May 1997.
- [12] B. K. Johnson and G. Venkataramanan, "A Hybrid Solid State Phase Shifter Using PWM AC-AC Converters," *IEEE Transactions on Power Delivery*, Oct 1998
- [13] S. Srinivasan and G. Venkataramanan, "Comparative Evaluation of PWM AC-AC Converters," *IEEE PESC Record*, Atlanta, GA, June 1995.
- [14] *Study of PWM AC-AC Converters for Custom Power*, EPRI TR-105601, Project 3389-17, Final Report, 1996.
- [15] Col. W. T. McLyman, *Transformer and Inductor Design Handbook*, 2nd ed., Marcel Dekker, New York, 1993.